Materials Horizons

Tunable Thermoplastic Elastomer Gels Derived from Controlled-Distribution Triblock Copolymers with Crystallizable Endblocks

Journal:	*Materials Horizons*
Manuscript ID	MH-COM-07-2023-001018.R1
Article Type:	Communication
Date Submitted by the Author:	07-Aug-2023
Complete List of Authors:	Hames, Nathan; North Carolina State University at Raleigh, Department of Chemical and Biomolecular Engineering Balsbough, Drew; North Carolina State University at Raleigh, Department of Chemical and Biomolecular Engineering Yan, Jiaqi; North Carolina State University at Raleigh, Department of Chemical and Biomolecular Engineering Wu, Siyu; Argonne National Laboratory Zuo, Xiaobing; Argonne National Laboratory Spontak, Richard; North Carolina State University at Raleigh, Department of Chemical and Biomolecular Engineering

Tunable Thermoplastic Elastomer Gels Derived from Controlled-Distribution Triblock Copolymers with Crystallizable Endblocks

Nathan T. Hames,[1] Drew Balsbough,[1] Jiaqi Yan,[1] Siyu Wu,[2] Xiaobing Zuo[2] and Richard J. Spontak[1,3]

[1]Department of Chemical & Biomolecular Engineering, North Carolina State University, Raleigh, NC 27695, USA

[2]Advanced Photon Source, Argonne National Laboratory, Lemont, IL 60439, USA

[3]Department of Materials Science & Engineering, North Carolina State University, Raleigh, NC 27695, USA

New Concepts

A thermoplastic elastomer (TPE) has been developed from a triblock copolymer with crystallizable polyethylene endblocks and a composition-adjustable random-copolymer midblock composed of polystyrene and hydrogenated polybutadiene – poly(ethylene-co-butylene). The crystallizable endblocks form more mechanically robust physical crosslinks that do not suffer from aging, and the random-copolymer midblock can be tuned to control the degree of thermodynamic incompatibility between the blocks and the lower glass transition temperature of the TPE.

Organogels prepared from this TPE archetype benefit tremendously from possessing crystallizable physical crosslinks and retaining their highly desirable attribute associated with composition-tunable properties for passive and dynamic technologies. Since the styrenic units reside in the midblock of the TPE, electron microscopy can be used to uniquely elucidate the spatial distribution of the midblocks, as well as reveal their conformations, as the organogel morphologies evolve from having embedded to surface-decorated crystals with changing composition. Preparation of organogels from the TPEs significantly enhances their mechanical properties over a finite composition range, and the G'–G" crossover evaluated by dynamic rheology corresponds to the endblock melting temperature discerned from calorimetry to mean that these materials can be melt-processed as structureless liquids at elevated temperatures.

Tunable Thermoplastic Elastomer Gels Derived from Controlled-Distribution Triblock Copolymers with Crystallizable Endblocks

Nathan T. Hames,[1†] **Drew Balsbough**,[1‡] **Jiaqi Yan**,[1§] **Siyu Wu**,[2] **Xiaobing Zuo**[2] and **Richard J. Spontak**[1,3*]

[1]Department of Chemical & Biomolecular Engineering, North Carolina State University, Raleigh, NC 27695, USA

[2]Advanced Photon Source, Argonne National Laboratory, Lemont, IL 60439, USA

[3]Department of Materials Science & Engineering, North Carolina State University, Raleigh, NC 27695, USA

ABSTRACT

Thermoplastic elastomers (TPEs) constitute an important category of triblock copolymers and are employed alone or upon physical modification with a midblock-selective oil (to form TPE gels, TPEGs) in a wide range of technologies. While most copolymers in this class of self-networking macromolecules possess glassy polystyrene endblocks and a rubbery polydiene or polyolefin midblock, we investigate TPEGs fabricated from a novel controlled-distribution copolymer with crystallizable polyolefin endblocks and a random-copolymer midblock. According to both electron microscopy and small-angle scattering, the morphologies of these TPEGs remain largely invariant up to 40 wt% oil and then transform considerably at higher oil levels. Although reductions in

† Current address: QC Chemistry Department, Pfizer, Rocky Mount, NC 27804, USA.
‡ Current address: Consulting Department, Deloitte, Charlotte, NC 28202, USA.
§ Current address: Kraton Innovation Center, Kraton Corporation, Houston, TX 77084, USA.
* To whom correspondence should be addressed (e-mail: Rich_Spontak@ncsu.edu).

endblock melting point and crystallinity measured by thermal calorimetry accompany increasing oil content, mechanical properties such as the uniaxial strain at break and fracture toughness improve in some cases by over 50% between 5 and 40 wt% oil. In fact, the strain at break can reach 2500% within this range, thereby confirming that (*i*) the structure-property relationships of these unique TPEGs are highly composition-tunable and (*ii*) these TPEGs, stabilized by crystallizable endblocks, provide an attractive alternative for ultrasoft and stretchy recyclable materials.

Introduction

Elastomers are becoming increasingly important for ubiquitous technologies requiring relatively low-modulus, lightweight and stretchy materials.[1] While polydiene, polyolefin and polysiloxane elastomers can be formulated with substantial property versatility[2] and are frequently employed for this reason to satisfy the property requirements of such applications, they are all chemically (i.e., permanently) crosslinked,[3] which commonly translates into microrubber particles during use and/or solid waste after use.[4] In contrast, thermoplastic elastomers (TPEs), originally envisaged as synthetic rubber, typically consist of block copolymers that self-organize into a soft rubbery network stabilized by rigid microdomains, which serve as physical crosslinks, and afford a recyclable and reusable alternative.[5,6] However, the functionality of TPEs, especially those

derived from styrenic triblock copolymers, can be greatly expanded through either chemical or physical means.[7] In this study, we focus exclusively on physically-modified TPEs comprised of nonpolar triblock copolymers imbibed with a midblock-selective, low-volatility oil. Such soft, elastomeric materials, referred to here as TPE gels (or TPEGs), are not limited by the chemistry-specific plateau modulus of the parent TPE and possess exquisitely composition-tunable mechanical properties.[8-11] For this reason, they are suitable for use not only in conventional technologies requiring media that provide vibration dampening or ballistic dissipation[12] but also as flexible electronics,[13] dielectric elastomers,[14,15] microfluidic substrates,[16] and shape-memory polymers.[17,18]

Most commercial TPEs are designed with polystyrene (S) endblocks and a polydiene or polyolefin midblock. While the midblock is rubbery and provides the desired elastic network, the endblocks normally self-assemble into glassy dispersions as either spheres or cylinders.[19,20] As glassy materials, these physical crosslinks suffer from the same shortcomings as other amorphous thermoplastics, including physical aging and solvent-induced plasticization. To circumvent such limitations, we turn our attention to TPEs designed and synthesized with crystallizable high-density polyethylene (E) endblocks.[21-27] This presents a second challenge (and opportunity) due to

the chemistry of the midblock, which normally starts as polybutadiene but becomes poly(ethylene-*co*-butylene) (EB) upon hydrogenation, intended to promote long-term stability. The ability of an AB-type block copolymer to microphase-separate generally depends on the thermodynamic incompatibility (χN, where χ denotes the Flory-Huggins interaction parameter between the A and B species and N represents the number of statistical units along the copolymer backbone) and the copolymer composition.[19,28] Since E and EB blocks are only slightly chemically different (very low χ), N must be relatively large for the blocks to self-organize into a nanostructure. High-molecular-weight block copolymers can, however, be difficult to process due to melt viscosity and molecular diffusion considerations, and they frequently do not produce equilibrated morphologies.

An alternative strategy relies on chemical modification of the EB midblock through the random incorporation of S units to yield a controlled-distribution block copolymer[29] (also known as a block random copolymer[30-33]) possessing a tunable S-*r*-EB (SEB) midblock. In this scenario, χ is replaced by a composition-dependent effective χ that takes into account the composition of each block. This largely unexplored synthetic approach affords three significant benefits: (1) χ is increased so that N does not have to be intolerably large to ensure microphase separation; (2) as a consequence, the order-disorder transition (ODT) temperature can be controlled by the S level in

the midblock; and (3) the glass transition temperature (T_g) of the midblock can likewise be regulated according to the midblock composition. In this study, we examine the morphologies and thermo-mechanical properties of a series of TPEGs prepared from a model ESEBE triblock copolymer.

Experimental

Materials

The ESEBE copolymer examined here was synthesized by living anionic polymerization and kindly provided in pellet form by the Kraton Corporation (Houston, TX). Its chemical structure is illustrated in **Scheme 1**. According to previous high-temperature size-exclusion chromatography,[27] the number-average molecular weight and dispersity of the copolymer were 145 kDa and 1.45, respectively, and the relevant copolymer compositions were 33 wt% E endblock and 22.5 wt% S in the SEB midblock. Reagent-grade toluene was procured from Fischer Scientific (Pittsburgh, PA), and a midblock-selective mineral oil (MO, Hydrobrite 380) was obtained from Sonneborn (Parsippany, NJ). In addition, ruthenium tetroxide (RuO_4, 0.5 wt% aqueous solution), a selective staining agent, was purchased from Electron Microscopy Sciences (Hatfield, PA). All materials and chemicals were used as-received.

Methods

Predetermined masses of ESEBE copolymer, MO and toluene were added together to a round-bottom flask, which was equipped with a condenser to avoid premature solvent evaporation and heated to 96 ˚C in a temperature-controlled oil bath to dissolve the copolymer. Oil loading levels (ϕ, in wt%) ranged from 0 to 80 wt% relative to the copolymer. [At ϕ above 80 wt%, the films were no longer form-stable and displayed visible evidence of flow.] Each solution was cast into a Teflon mold and permitted to dry quiescently (in a glass chamber located in a fume hood) for 1 week at 22 ˚C. Resultant films intended for mechanical property testing were subsequently melt-pressed at 160 ˚C for 5 min, followed by slow cooling to ambient temperature. In all cases, the films became increasingly visually transparent and tacky with increasing ϕ.

Specimens for transmission electron microscopy (TEM) were cryoultramicrotomed at –100 ˚C, and electron-transparent sections were collected on carbon-coated Cu grids and subjected to RuO_4(aq) vapor for 7 min to stain the styrenic units in the copolymer midblock. Bright-field images were acquired on a Hitachi HT7800 electron microscope operated at an accelerating voltage of 80 kV. Complementary wide- and small-angle X-ray scattering (WAXS and SAXS, respectively) was

performed on beamline 12-ID-B of the Advanced Photon Source at Argonne National Laboratory. Films were exposed to a 13.3 keV beam with a wavelength (λ) of 0.0932 nm at a flux of ~10^{12} photons/s for 1 s. The resulting 2D scattering patterns were azimuthally integrated to yield intensity profiles as a function of the scattering vector (q), where $q = (4\pi/\lambda)\sin\theta$ and θ represents the scattering half-angle. To evaluate the thermal properties, differential scanning calorimetry (DSC) was conducted on a TA Instruments Q100 instrument operated at a heating rate of 20 ˚C/min and a cooling rate of 20 ˚C/min in a nitrogen atmosphere. Quasi-static uniaxial tensile behavior was measured on a Universal Machine 5943 (Instron) load frame at ambient temperature and constant crosshead speed to evaluate important mechanical properties at different ϕ. Film thicknesses were measured with a digital thickness gauge. Dynamic shear rheology was similarly performed on an Anton Paar MCR 302 rheometer equipped with parallel plates to ascertain the influence of ϕ on (*i*) network characteristics as a function of oscillatory frequency (ω) under isostrain (1%) and isothermal (25 ˚C) conditions and (*ii*) thermal characteristics as a function of temperature (T) under isostrain (1%) and isochronal (0.1 rad/s) conditions.

Results and Discussion

Previously, we investigated[27] the competitive effects of self-assembly and crystallization with regard to ESEBE copolymers to discern if the crystallization-directed self-assembly (CDSA) mechanism introduced by Manners and co-workers[34,35] applied to two ESEBE copolymers as they precipitated from a selective solvent upon cooling. The corresponding TEM images revealed that the copolymers formed irregularly-shaped 3D aggregates consisting of acicular crystals whose orientation was affected by the periphery of the aggregates. According to the series of TEM images presented in **Figure 1a**, such surface effects are not apparent in the bulk morphologies of the TPEG films. Up to 40 wt% MO, the morphologies are strikingly similar, generally composed of light (unstained) elongated features, presumed to be endblock crystals measuring 7-10 nm across, embedded in a dark (stained) matrix, attributed to the MO-swollen copolymer midblock. Although the crystals are not highly ordered, they nonetheless display evidence of limited correlation, yielding a periodicity (D) of 18-21 nm. It is important to recognize that, within this relatively low range of ϕ, the crystals are sufficiently close to each other so that the matrix consists of both bridged and looped midblock populations,[20,36] as depicted in **Figure 1b**. When ϕ is increased to 60 wt% in **Figure 1a**, however, the morphology changes so that the crystals appear outlined (in projection) within a lighter matrix. This scenario corresponds to the high-ϕ illustration provided in

Figure 1b, wherein the population of midblock bridges decreases significantly and midblock loops effectively decorate the surface of each crystal. Upon further increasing ϕ to 80 wt% in **Figure 1a**, the morphology transforms into flocs or a defective network without distinguishable crystals.

The series of TEM images in **Figure 1a** is likewise consistent with the systematic evolution of a network to discrete flocs predicted[37] by computer simulations of molecularly asymmetric A_1BA_2 copolymers, with endblocks differing in size, as the A_2 block is progressively shortened. Complementary SAXS profiles are included in **Figure 1c** and confirm that the TPE and TPEG morphologies are not highly ordered (due to the lack of well-defined and numerous scattering peaks) but remain surprisingly similar up to 40 wt% MO. Within this composition range, values of D calculated from the position of the principal peak (at q*) in conjunction with Bragg's law ($D = 2\pi/q^*$) range from 26 to 30 nm, in close agreement with measurements extracted from TEM images. Another feature of interest up to 40 wt% MO is the ratio of the second scattering peak to q*, which can be used to assess the overall symmetry of the nanostructure. From the 4 low-ϕ scattering profiles in **Figure 1c**, this ratio is an integer (3.03 ± 0.04), implying that the morphology is likely planar because of the acicular endblock crystals. As ϕ is increased to 60 wt% MO, q* shifts to a lower value due to swelling, resulting in an increase in D to 36 nm, whereas the peak

ratio changes to ~3.33 (the second peak, while broader than the ones in the profiles at lower ϕ, nonetheless remains discernible). At 80 wt% MO, q* shifts further, yielding D ≈ 52 nm (a ~2x increase relative to the neat copolymer) without a clearly defined second peak, indicating that the nanostructure exhibits no long-range order (in agreement with the TEM images in **Figure 1a**).

The thermal characteristics of the ESEBE TPEGs are apparent in the DSC thermograms measured at different ϕ in **Figure 2a**. These results confirm that all the TPEGs examined here (up to 80 wt% MO) possess crystallinity, as evidenced by the endotherms that systematically shift to lower temperature with increasing ϕ. Complementary findings from WAXS (data not shown) likewise verify that the (110) and (200) crystal peaks are similarly present for all the TPEGs. The normal melting point (T_m) is determined from the peak position of each endotherm and is displayed as a function of ϕ in **Figure 2b** for specimens after drying (solution-crystallized) and after a second DSC heating cycle (melt-crystallized). The observation that the two different process histories yield comparable T_m values suggests that crystallization is insensitive to these solidification processes, although the thickness of the crystalline lamellae (L) is related to T_m by the Gibbs-Thomson equation (without considering curvature or confinement effects[38]). Assuming that the surface energy, density and heat of melting of the crystalline lamellae formed by the ESEBE

endblocks are all independent of ϕ, the ratio of L evaluated at 80 wt% MO to L at 5 wt% MO can be estimated from $[1 - T_m(\phi=5\%)/T_{m\infty}] / [1 - T_m(\phi=80\%)/T_{m\infty}]$, where $T_{m\infty}$ denotes T_m for the neat copolymer (at ϕ = 0 wt% MO). This calculation yields $L(\phi=80\%)/L(\phi=5\%) = 0.11$, which corroborates a substantial reduction in the thickness of the crystalline lamellae at high ϕ. The degree of crystallinity (X_c) ascertained from the specific heat of melting (the area under each melting endotherm) after corrected for composition and normalized to 100% crystalline polyethylene[39] (~300 J/g) affords a measure of the extent to which the copolymer molecules crystallize and is likewise provided as a function of ϕ in **Figure 2c**. Independent measurements of X_c extracted from WAXS profiles are included for comparison in **Figure 2c** to demonstrate favorable agreement. Taken together, this collection of data indicates that solution crystallization facilitates the formation of crystals relative to melt crystallization over the range of ϕ examined, and X_c remains relatively constant (or increases slightly) with increasing ϕ up to 60 wt% MO and then drops when discrete crystals are no longer evident at 80 wt% MO.

While the morphologies and thermal characteristics of ESEBE-derived TPEGs presented in **Figures 1** and **2**, respectively, are important to establish important structure-property relationships, we now consider the dependence of mechanical properties on ϕ. The results from uniaxial tensile

tests are displayed in **Figure 3a** and confirm that the strain response of these TPEGs is very sensitive to ϕ, with the maximum strain at break (ε_{max}) increasing from ~1400% for the neat copolymer to ~2500% at 40 wt% MO. To determine if the mechanical properties of these TPEGs are similar to those exhibited by styrenic TPEs, we include the tensile modulus (E), tested in at least triplicate, as a function of copolymer content ($100 - \phi$) in **Figure 3b**. The outcome reveals that $E \sim (100 - \phi)^{\alpha}$, where $\alpha = 2.64$, which is slightly higher than $\alpha \approx 2$ (indicating that E is governed by midblock entanglements[40]) reported for many styrenic TPEGs. Two other properties of particular interest here are ε_{max} and the fracture toughness computed from the area under the stress-strain curve. These metrics, normalized with respect to their respective values measured for the oil-free TPE to obtain relative values, are provided in **Figure 3c** and demonstrate that both properties are substantially improved, by more than 50% in some cases, from 5 to 40 wt% MO. According to **Figures 1a** and **1c**, the TPEG morphologies within this composition range consist of acicular endblock crystals embedded within a MO-swollen matrix comprised of both bridged and looped copolymer midblocks (depicted in **Figure 1b**). At higher ϕ, the midblock network weakens as the population of midblock bridges decreases, and both relative properties in **Figure 3c** drop below unity. Taken together, **Figures 1** and **3c** directly establish structure-property relationships.

The dependence of the dynamic moduli (G', the storage modulus, and G", the loss modulus) on ω in **Figure 3d** verifies that, at ambient temperature, G' is consistently greater than G", as well as nearly independent of ω, over the entire ω range examined. This rheological signature is indicative of network behavior. On one hand, G' decreases systematically with increasing ϕ, in agreement with intuitive expectation and the tensile moduli shown in **Figure 3b**. On the other hand, G", which also decreases, becomes increasingly ω-dependent as ϕ is increased (and the TPEG network weakens or transforms altogether at 80 wt% MO) in **Figure 3d**. Additional property insights gleaned from the tensile and rheological data reported here are presented in **Figures S1-S3** of the **Supplementary Information**. In **Figure 3e**, we explore the effect of raising T from 50 to 150 ˚C on both moduli under isochronal conditions at two different ϕ levels (0 and 20 wt% MO). At low T, G' > G" and the TPEGs behave solid-like (as expected from **Figure 3d**). A crossover occurs where G' = G" upon heating to an intermediate T ($T_{G'=G"}$), beyond which G" > G' and the specimens behave increasingly liquid-like with tanδ (= G"/G') systematically decreasing with increasing T. Although not included here, all the TPEGs produced in this study exhibit similar behavior, but the experimental scatter in G' and G" at low and high T increase as ϕ is increased beyond 20 wt% MO. Values of $T_{G'=G"}$ extracted from these rheological results are displayed as a

function of T_m from calorimetry in **Figure 3f** and reveal excellent agreement up to 70 wt% MO (only the TPEG with 80 wt% MO deviates significantly), implying that the rheological crossover can be attributed to crystal melting. Unlike TPEGs derived from high-molecular-weight styrenic TPEs, these TPEGs do not exhibit any evidence of an ODT transition, in which case they should be melt-processable as single-phase liquids at $T > T_m$.

Conclusions

The objective of this study is to examine the morphological and property development of TPEGs produced from a controlled-distribution ESEBE triblock copolymer with crystallizable endblocks, which are expected to be more stable (by preventing chain pullout and microdomain hopping) than the glassy endblocks associated with styrenic TPEs. According to TEM images, the morphologies of these unique TPEGs indicate that, up to ~40 wt% oil, acicular endblock crystals are embedded in a swollen matrix composed of midblock bridges and loops. At higher oil levels, the copolymer nanostructure clearly transforms, ultimately yielding a high defective network or a series of flocs. Complementary results acquired by SAXS corroborate this morphological progression and suggest that, on the basis of scattering peak positions, the morphology is best

described as planar at low oil content. Thermal calorimetry confirms that both the melt temperature and degree of crystallinity decrease with increasing oil fraction and that endblock crystallinity is detected up to 80 wt% oil. Quasistatic tensile tests demonstrate that the maximum strain at break and fracture toughness increase substantially upon addition of up to 40 wt% oil. Beyond this limit, the mechanical properties of the TPEGs are compromised. Dynamic rheology verifies that these materials possess load-bearing networks and that the solid→liquid transition coincides with the melting temperature measured by calorimetry. Several important structure-property relationships identified here are compiled in **Table 1**. Since TPEGs are suitable for use as soft materials in a wide variety of technologies requiring composition-tunable morphologies and properties, the crystallizable TPEGs investigated here provide an attractive alternative to applications that are adversely affected by the use of styrenic TPEGs. For example, styrenic TPEGs constitute excellent anthropomorphic surrogates with electromechanical properties comparable to mammalian skeletal muscle,[14] and they are likewise suitable for transdermal drug delivery.[41] Crystallizable TPEGs are anticipated to improve these uses through enhanced stability. Moreover, these materials provide a rare opportunity to visualize the midblock of triblock copolymer systems and, by doing so, explore the direct relation between midblock conformations and their desirable mechanical properties.

Acknowledgments

This study was supported by the Kraton Corporation and used instrumentation maintained in the NC State Analytical Instrumentation Facility (AIF) with support from the National Science Foundation (ECCS-2025064). The AIF is a member of the North Carolina Research Triangle Nanotechnology Network (RTNN), a site in the National Nanotechnology Coordinated Infrastructure (NNCI). This research used resources of the Advanced Photon Source, a U.S. Department of Energy (DOE) Office of Science User Facility operated for the DOE Office of Science by Argonne National Laboratory under Contract No. DE-AC02-06CH11357. The authors are grateful to Dr. J. E. Flood for providing the copolymer and Drs. A. J. Bell and M. Shamsi for technical assistance.

Conflict of Interest

The authors confirm that they have no conflict of interest with regard to this work.

References

1. Rogers, J. A.; Someya, T.; Huang, Y. Materials and Mechanics for Stretchable Electronics. *Science* **2010**, *327*, 1603.

2. Wolf, M. P.; Salieb-Beugelaar, G. B.; Hunziker, P. PDMS with Designer Functionalities—Properties, Modifications Strategies, and Applications. *Prog. Polym. Sci.* **2018**, *83*, 97.

3. Zhong, M.; Wang, R.; Kawamoto, K.; Olsen, B. D.; Johnson, J. A. Quantifying the Impact of Molecular Defects on Polymer Network Elasticity. *Science* **2016**, *353*, 1264.

4. Hall, L. L.; Palmqvist, A.; Kampmann, K.; Khan, F. R. Ecotoxicology of Micronized Tire Rubber: Past, Present and Future Considerations. *Sci. Total Environ*. **2020**, *706*, 135694.

5. Holden, G.; Kricheldorf, H. R.; Quirk, R. P. *Thermoplastic Elastomers*, *3rd ed*.; Hanser: Munich, **2004**.

6. Wang, W.; Lu, W.; Goodwin, A.; Wang, H.; Yin, P.; Kang, N.-G.; Hong, K.; Mays, J. W. Recent Advances in Thermoplastic Elastomers from Living Polymerizations: Macromolecular Architectures and Supramolecular Chemistry. *Prog. Polym. Sci.* **2019**, *95*, 1.

7. Yan, J.; Spontak, R. J. Advances in Stimuli-Responsive and Functional Thermoplastic Elastomers. In *Elastomer Blends and Composites: Principles, Characterizations, Advances and Applications* (M. R. Sanjay, J. Parameswaranpillai, S. Siengchin, and T. Ozbakkaloglu, eds.), Elsevier: Amsterdam; **2022**, pp. 353-404.

8. Laurer, J. H.; Mulling, J. F.; Khan, S. A.; Spontak, R. J.; Bukovnik, R. Thermoplastic Elastomer Gels: I. Effects of Composition and Processing on Morphology and Gel Behavior. *J. Polym. Sci. B: Polym. Phys.* 1998, *36*, 2379.

9. Krishnan, A. S.; Smith, S. D.; Spontak, R. J. Ternary Phase Behavior of a Triblock Copolymer in the Presence of an Endblock-Selective Homopolymer and a Midblock-Selective Oil. *Macromolecules* 2012, *45*, 6056.

10. Mishra, S.; Prado, R. M. B.; Zhang, S.; Lacy, T. E.; Gu, X.; Kundu, S. Mechanical Properties and Failure Behavior of Physically Assembled Triblock Copolymer Gels with Varying Midblock Length. *J. Polym. Sci. B: Polym. Phys.* 2019, *57*, 1014.

11. Mineart, K. P.; Vallely, M. J.; Rankin, L. A.; Hill, D. M.; Lee, B. Implications of Styrenic Triblock Copolymer Gel Mechanics on Midblock Bridging Fraction. *Polymer* 2022, *260*, 125394.

12. Mrozek, R. A.; Leighliter, B.; Gold, C. S.; Beringer, I. R.; Yu, J. H.; VanLandingham, M. R.; Moy, P.; Foster, M. H.; Lenhart, J. L. The Relationship Between Mechanical Properties and Ballistic Penetration Depth in a Viscoelastic Gel. *J. Mech. Behav. Biomed. Mater*. **2015**, *44*, 109.

13. Mineart, K. P.; Yiliang, L.; Desai, S. C.; Krishnan, A. S.; Spontak, R. J.; Dickey, M. D. Ultrastretchable, Cyclable and Recyclable 1- and 2-Dimensional Conductors Based on Physically Cross-linked Thermoplastic Elastomer Gels. *Soft Matter* **2013**, *9*, 7695.

14. Shankar, R.; Ghosh, T. K.; Spontak, R. J. Electroactive Nanostructured Polymers as Tunable Actuators. *Adv. Mater.* **2007**, *19*, 2218.

15. Lau, G. K.; Ren, Z. X.; Chiang, K. T. Effect of Stretch Limit Change on Hyperelastic Dielectric Actuation of Styrene-Ethylene/Butylene-Styrene (SEBS) Copolymer Organogels. *Smart Mater. Struct.* **2022**, *31*, 095019.

16. Sudarsan, A. P,; Wang, J.; Ugaz, V. M. Thermoplastic Elastomer Gels: An Advanced Substrate for Microfluidic Chemical Analysis Systems. *Anal. Chem.* **2005**, *77*, 5167.

17. Q. Zhang, S. Song, J. Feng, P. Wu, A New Strategy to Prepare Polymer Composites with Versatile Shape Memory Properties. *J. Mater. Chem.* **2012**, *22*, 24776.

18. Mineart, K. P.; Tallury, S. S.; Li, T.; Lee, B.; Spontak, R. J. Phase-Change Thermoplastic Elastomer Blends for Tunable Shape Memory by Physical Design. *Ind. Eng. Chem. Res.* **2016**, *55*, 12590.

19. Matsen, M. W. Effect of Architecture on the Phase Behavior of AB-Type Block Copolymer Melts. *Macromolecules* **2012**, *45*, 2161.

20. Tallury, S. S.; Spontak, R. J.; Pasquinelli, M. A. Dissipative Particle Dynamics of Triblock Copolymer Melts: A Midblock Conformational Study at Moderate Segregation. *J. Chem. Phys.* **2014**, *141*, 244911.

21. Grassi, A.; Caprio, M.; Zambelli, A.; Bowen, D. E. Synthesis and Characterization of Syndiotactic Styrene−Ethylene Block Copolymers. *Macromolecules* **2000**, *33*, 8130.

22. Schmalz, H.; Böker, A.; Lange, R.; Krausch, G.; Abetz, V. Synthesis and Properties of ABA and ABC Triblock Copolymers with Glassy (A), Elastomeric (B), and Crystalline (C) Blocks. *Macromolecules* **2001**, *34*, 8720.

23. Myers, S. B.; Register, R. A. Extensibility and Recovery in a Crystalline−Rubbery−Crystalline Triblock Copolymer. *Macromolecules* **2009**, *42*, 6665.

24. Zuo, F.; Alfonzo, C. G.; Bates, F. S. Structure and Mechanical Behavior of Elastomeric Multiblock Terpolymers Containing Glassy, Rubbery, and Semicrystalline Blocks. *Macromolecules* **2011**, *44*, 8143.

25. Petzetakis, N.; Stone, G. M.; Balsara, N. P. Synthesis of Well-Defined Polyethylene-Polydimethylsiloxane-Polyethylene Triblock Copolymers by Diimide-Based Hydrogenation of Polybutadiene Blocks. *Macromolecules* **2014**, *47*, 4151.

26. Burns, A. B.; Register, R. A. Thermoplastic Elastomers via Combined Crystallization and Vitrification from Homogeneous Melts. *Macromolecules* **2016**, *49*, 269.

27. Yan, J.; Lee, B.; Smith, S. D.; Spontak, R. J. Morphological Studies of Solution-Crystallized Thermoplastic Elastomers with Polyethylene Endblocks and a Random-Copolymer Midblock. *Macromol. Rapid Commun*. **2021**, *42*, 2100442.

28. Bates, F. S.; Fredrickson, G. H. Block Copolymers — Designer Soft Materials. *Phys. Today* **1999**, *52*, 32.

29. Yang, J.; Germack, D. S.; Spontak, R. J. Characterization of Controlled-Distribution Hydrogenated Styrenic Block Copolymers by NMR Spectroscopy. *ACS Appl. Polym. Mater*. **2023** (in press).

30. Staudinger, U.; Satapathy, B. K.; Thunga, M.; Weidisch, R.; Janke, A.; Knoll, K. Enhancement of Mechanical Properties of Triblock Copolymers by Random Copolymer Middle Blocks. *Eur. Polym. J.* **2007**, *43*, 2750.

31. Beckingham, B. S.; Register, R. A. Synthesis and Phase Behavior of Block-Random Copolymers of Styrene and Hydrogenated Isoprene. *Macromolecules* **2011**, *44*, 4313.

32. Flood, J. E.; Tan, K.; Muyldermans, X.; McGilbert, S. K.; Culbert, L. A New Semi-Crystalline Styrenic Block Copolymer for Elastic Films, Fibers and Compounds. Presented at the 2017 SPE International Polyolefins Conference, Houston, TX, 2017.

33. Ashraf, A. R.; Ryan, J. J.; Satkowski, M. M.; Lee, B.; Smith, S. D.; Spontak, R. J. Bicomponent Block Copolymers Derived from One or More Random Copolymers as an Alternative Route to Controllable Phase Behavior. *Macromol. Rapid Commun.* **2017**, *38*, 1700207.

34. Wang, X.; Guerin, G.; Wang, H.; Wang, Y.; Manners, I.; Winnik, M. A. Cylindrical Block Copolymer Micelles and Co-Micelles of Controlled Length and Architecture. *Science* **2007**, *317*, 644.

35. Gädt, T.; Ieong, N. S.; Cambridge, G.; Winnik, M. A.; Manners, I. Complex and Hierarchical Micelle Architectures from Diblock Copolymers Using Living, Crystallization-Driven Polymerizations. *Nat. Mater.* **2009**, *8*, 144.

36. Yan, J.; Tuhin, M. O.; Sadler, J. D.; Smith, S. D.; Pasquinelli, M. A.; Spontak, R. J. Network Topology and Stability of Homologous Multiblock Copolymer Physical Gels. *J. Chem. Phys.* **2020**, *153*, 124904.

37. Tallury, S. S.; Mineart, K. P.; Woloszczuk, S.; Williams, D. N.; Thompson, R. B.; Pasquinelli, M. A.; Banaszak, M.; Spontak, R. J. Molecular-Level Insights into Asymmetric Triblock Copolymers: Network and Phase Development. *J. Chem. Phys.* **2014**, *141*, 121103.

38. Svintradze, D. V. Generalization of Young-Laplace, Kelvin, and Gibbs-Thomson Equations for Arbitrarily Curved Surfaces. *Biophys. J.* **2023**, *122*, 892.

39. Mirabella, F. M.; Bafna, A. Determination of the Crystallinity of Polyethylene/a-olefin Copolymers by Thermal Analysis: Relationship of the Heat of Fusion of 100% Polyethylene Crystal and the Density. *J. Polym. Sci. B: Polym. Phys.* **2002**, *40*, 1637.

40. Vega, D. A.; Sebastian, J. M.; Loo, Y. L.; Register, R. A. Phase Behavior and Viscoelastic Properties of Entangled Block Copolymer Gels. *J. Polym. Sci. B: Polym. Phys.* **2001**, *39*, 2183.

41. Mineart, K. P.; Hong, C.; Rankin, L. A. Decoupling of Mechanical and Transport Properties in Organogels via Solvent Variation. *Gels* **2021**, *7*, 61.

Table 1. Qualitative summary of structure-property relationships in ESEBE-based TPEGs relative to the parent ESEBE copolymer.

Oil fraction (wt%)	Network	Copolymer crystallinity	Maximum strain	Toughness	Appearance
5	Continuous	Similar	Improved	Improved	Opaque
20	Continuous	Similar	Improved	Improved	Opaque
40	Continuous	Similar	Improved	Improved	Semi-transparent
60	Transitional	Similar	Similar	Reduced	Semi-transparent/ transparent
80	Defective or flocs	Reduced	Reduced	Reduced	Transparent

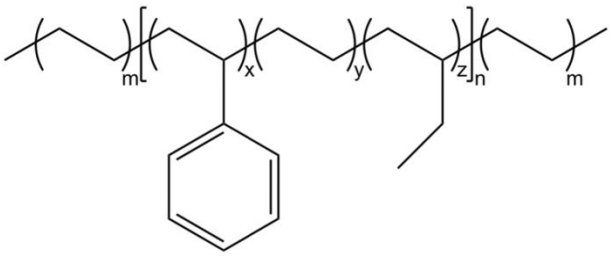

Scheme 1. Chemical structure of the ESEBE triblock copolymer.

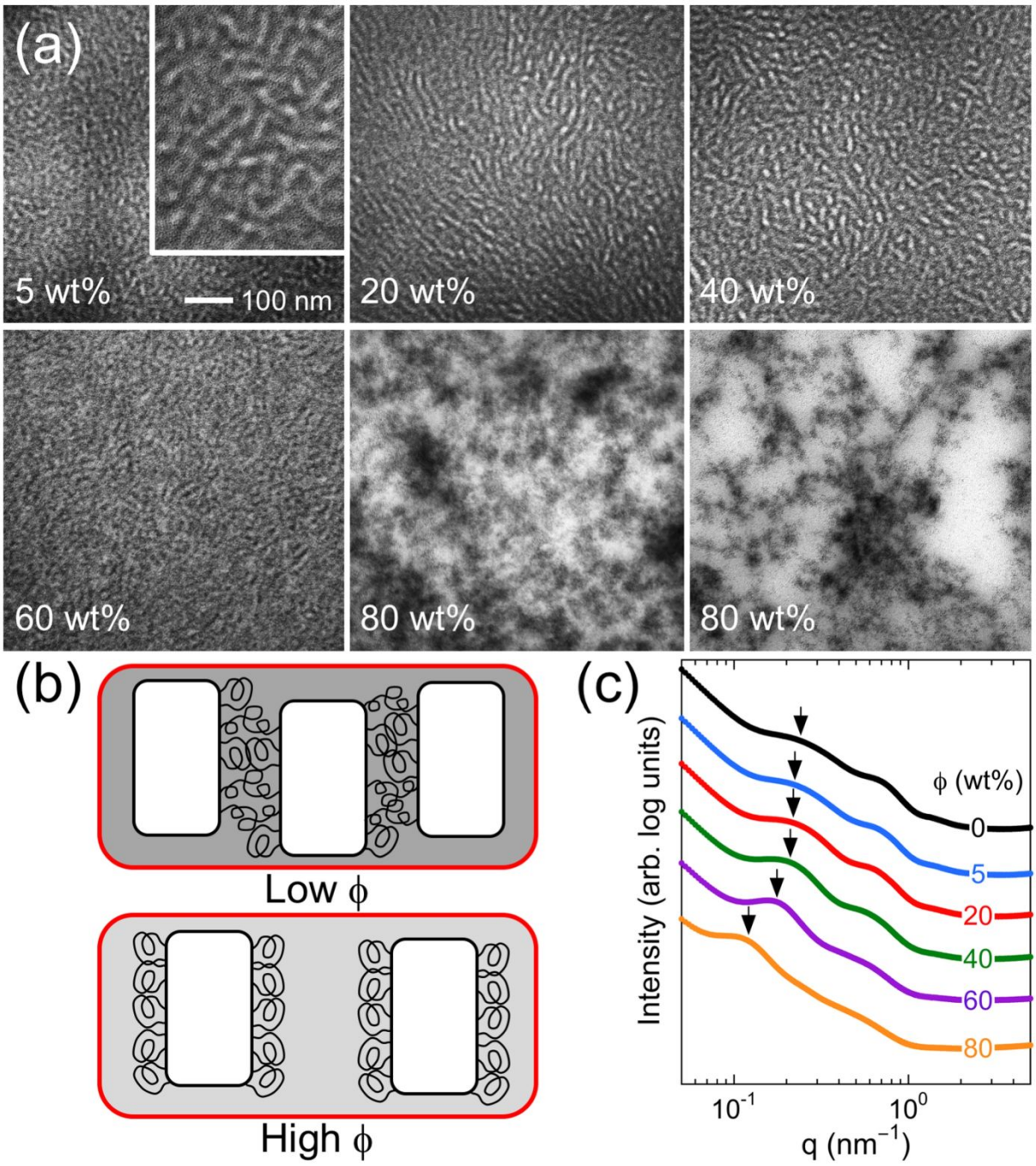

Figure 1. In (a), a series of TEM micrographs acquired from ESEBE-based TPEGs at different MO levels (ϕ, labeled). In these images, the styrene-containing midblocks are selectively stained and appear dark, and the inset included in the 5 wt% MO image is a 2x enlargement. Schematic illustrations of the midblock conformations at high and low ϕ levels (labeled) are provided in (b). Complementary SAXS intensity profiles are displayed as a function of wave vector (q) for TPEGs

differing in MO content (labeled and color-coded) in (c). The arrows identify the principal scattering peak in each profile.

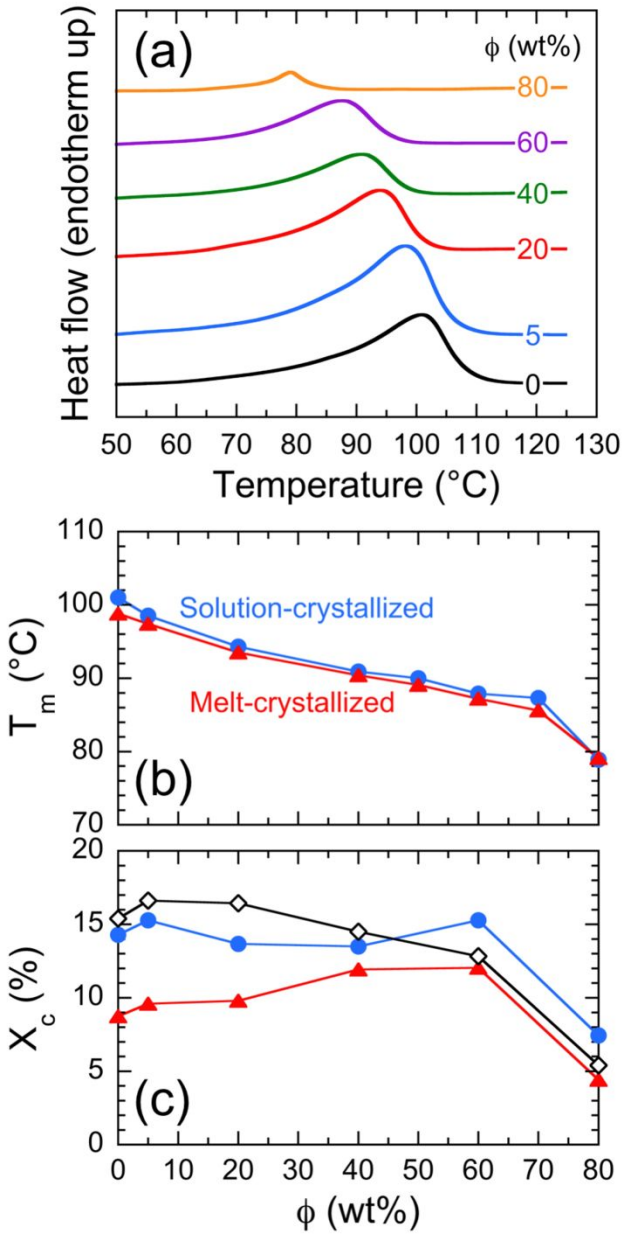

Figure 2. In (a), a series of DSC thermograms acquired from the neat ESEBE copolymer and its TPEGs at different ϕ (labeled and color-coded) after solution crystallization. Extracted values of (b) T_m and (c) X_c after solution (blue circles) and melt (red triangles) crystallization are provided as functions of ϕ. Included in (c) are results obtained by analyzing the crystal peaks in composition-corrected WAXS profiles (black diamonds). In (b) and (c), the solid lines serve to connect the data.

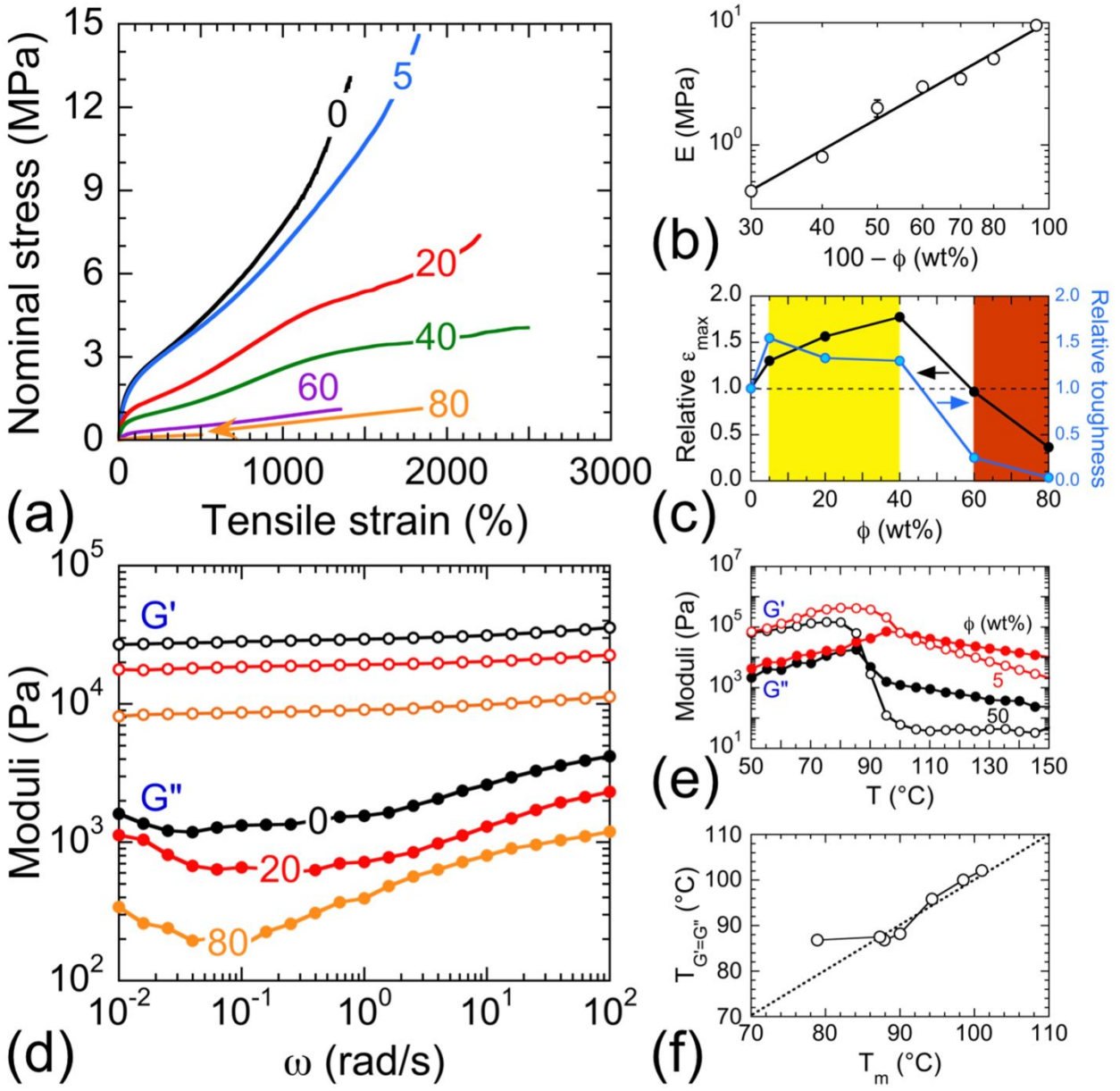

Figure 3. In (a), the response of the neat ESEBE copolymer and its TPEGs at different ϕ (in wt%, labeled and color-coded) to uniaxial tensile strain. The dependence of the tensile modulus (E) on copolymer content (100 – ϕ) in (b) reveals the existence of a scaling relationship (solid line), and relative values of the maximum strain (ε_{max}) and toughness are presented as functions of ϕ in (c). The yellow and red composition zones indicate where the properties are enhanced and compromised, respectively, and the solid lines serve to connect the data. The frequency (ω) spectra of the dynamic storage and loss shear moduli (G', open; G", filled) measured from the ESEBE copolymer and its TPEGs at two different ϕ (in wt%, labeled and color-coded) are provided in (d),

and the temperature dependence of the moduli for the copolymer and a TPEG with 20 wt% MO (labeled and color-coded) is included in (e). Values of the G'=G" crossover temperature are shown as a function of T_m from calorimetry in (f), and the dotted line indicates where $T_{G'=G"} = T_m$.